Available at
http://pvamu.edu/aam
Appl. Appl. Math.
ISSN: 1932-9466

Applications and Applied Mathematics:
An International Journal
(AAM)

Vol. 05, Issue 2 (December 2010), pp. 303 – 320
(Previously, Vol. 05, Issue 10, pp. 1400 – 1417)

Two-Layered Pulsatile Blood Flow in a Stenosed Artery with Body Acceleration and Slip at Wall

Devajyoti Biswas and Uday Shankar Chakraborty*
Department of Mathematics
Assam University
Silchar-788011, India
udayhkd@gmail.com

Received: January 23, 2010; Accepted: July 29, 2010

Abstract

Pulsatile flow of blood through an artery in presence of a mild stenosis has been investigated in this paper assuming the body fluid blood as a two-fluid model with the suspension of all the erythrocytes in the core region as Bingham Plastic and the peripheral region of plasma as a Newtonian fluid. This model has been used to study the influence of body acceleration, non-Newtonian nature of blood and a velocity slip at wall, in blood flow through stenosed arteries. By employing a perturbation analysis, analytic expressions for the velocity profile, Plug-core radius, flow rate, wall shear stress and effective viscosity, are derived. The variations of flow variables with different parameters are shown diagrammatically and discussed. It is noticed that velocity and flow rate increase but effective viscosity decreases, due to a wall slip. Flow rates and speed are enhanced further due to the influence of body acceleration.

Keywords: Pulsatile flow; Peripheral Plasma Layer (PPL); Velocity-slip; Body acceleration; Bingham Plastic; Stenosis

MSC 2010 No.: 76Z05, 74G10

1. Introduction

An abnormal growth, reducing the lumen of an artery is usually called a stenosis or an atherosclerosis [Young (1968); Sankar and Lee (2009); Biswas (2000); Biswas and Chakraborty

*Corresponding Author

(2009a); Biswas and Chakraborty (2009b)], which is one of the most widespread diseases that can cause serious circulatory disorders, by reducing or occluding the blood supply. For instance, stenosis in arteries supplying blood to brain, can bring about cerebral strokes, likewise, in coronary arteries, it can be myocardial infarction, leading to a heart failure [Sinha and Singh (1984)].

Several theoretical and experimental analyses were performed to study the blood flow characteristics in the presence of stenosis [McDonald (1979); Mandal (2005); Bali and Awasthi (2007); Biswas and Chakraborty (2009a); Biswas and Chakraborty (2009b); Sankar and Ismail (2009)]. It has been reported that though at high shear rates blood exhibits Newtonian character in large arteries like aorta [Taylor (1959)], blood being a suspension of corpuscles, at low shear rates and during its flow through narrow vessels, behaves like a non-Newtonian fluid [Merrill et al. (1965); Charm and Kurland (1974)].

Bugliarello and Sevilla (1970) and Cokelet (1972) have experimentally proved that for blood flowing through small vessels, there exists a cell-poor plasma (Newtonian fluid) layer and a core region of suspension of almost all the erythrocytes. Bugliarello and Sevilla (1970) presented the flow of blood in small diameter tubes by a two-layered model assuming peripheral and core fluids as Newtonian fluids of different viscosities. Following the experimentally verified model of Bugliorello and Sevilla (1970), two-fluid modeling of blood flow has been discussed and used by a good number of researchers. Shukla et al. (1980) applied a two-fluid model to discuss the flow of blood through a stenosis. Chaturani and Upadhya (1979, 1981) addressed the flow of blood in small diameter tubes using the two-layered model of Micropolar and Couple stress fluids respectively. Two-fluid model analyses have been carried out by Srivastava (2000) to observe the effects of a non-symmetrical stenosis on blood flow characteristics.

It has been pointed out by many investigators that under certain flow situations, blood possesses a finite yield stress [Fung (1981); Kapur et al. (1982)]. One interesting and specialized case of material with yield stress, is known as Bingham plastic whose consistency curve or, flow behaviour, is shown by a straight line curve [Fung (1981); Kapur et al. (1982)]. This particular material deforms elastically, until the yield stress is reached, but once this stress is exceeded, it flows as a Newtonian fluid, with shear stress being linearly related to rate of shear strain [Schlichting (1968)]. It therefore seems to be realistic, in considering blood behaving as a Bingham plastic in the core region of a constricted artery.

It is well known that blood flow in the human circulatory system is caused by the pumping action of the heart, which in turn produces a pressure gradient throughout the system [Fung (1981); Misra et al. (2008)]. Human heart is a muscular pump and due to contraction and expansion of heart muscles, there produces a pressure difference in its systolic and diastolic conditions, popularly known as pressure pulse which physicians check at the wrist. Flow of blood due to this pressure pulse, is known as pulsatile flow [Chaturani and Samy (1985); Guyton and Hall (2006)]. Again under exceptional circumstances, human body may also be subjected to accelerations (or vibrations). Accelerative disturbances are quite common in normal life, for example, while riding in a vehicle or while landing, taking off and flying in an aircraft or spacecraft, operating a jack hammer and, sudden and fast movements of the body, during gymnastics and sports activities. In such situations, human body may unintentionally be

subjected to external accelerations. The flow of blood in the arteries of such a subject is influenced by such whole body accelerations [Sud and Sekhon (1985, 1987)]. Though human body can adapt to changes, however prolonged exposures to such accelerative disturbances may lead to health problems, like headache, abdominal pain, loss of vision and increased pulse rate. Sud and Sekhon (1985) presented a mathematical model of blood flow in a single artery subject to pulsating pressure gradient as well as body acceleration. Nagarani and Sarojamma (2008) presented a theoretical model of pulsatile blood flow in a stenosed artery under the action of periodic body acceleration considering blood behaving as a Casson fluid.

In all the above mentioned studies, traditional no-slip boundary condition [Day (1990)] has been employed. However, a number of studies of suspensions in general and blood flow in particular both theoretical [Vand (1948); Jones (1966); Nuber (1967); Brunn (1974); Chaturani and Biswas (1984)] and experimental [Bugliarello and Hayden (1962); Bennet (1967)], have suggested the likely presence of slip (a velocity discontinuity) at the flow boundaries (or in their immediate neighbourhood). Recently, Misra and Shit (2007), Ponalgusamy (2007), Biswas and Chakraborty (2009a, 2009b, 2010) have developed mathematical models for blood flow through stenosed arterial segment, by taking a velocity slip condition at the constricted wall. Thus, it seems that consideration of a velocity slip at the stenosed vessel wall will be quite rational, in blood flow modeling.

With the above motivations, an attempt has been made to study the effects of slip (at the stenotic wall) and the influence of body acceleration, on the flow variables (wall shear stress, velocity profiles, flow rate and effective viscosity) for two layered pulsatile blood flow through a constricted vessel.

2. Mathematical Formulation

We consider an axially symmetric, laminar, pulsatile and fully developed flow of blood (assumed to be incompressible) through a circular tube with an axially symmetric mild stenosis as shown in Fig. 1. It is assumed that the wall of the tube is rigid and the body fluid blood is represented by a two-fluid model with a core region of suspension of all erythrocytes as a Bingham plastic fluid and a peripheral layer of plasma as a Newtonian fluid. The artery length is assumed to be large enough as compared to its radius so that the entrance and exit, special wall effects can be neglected.

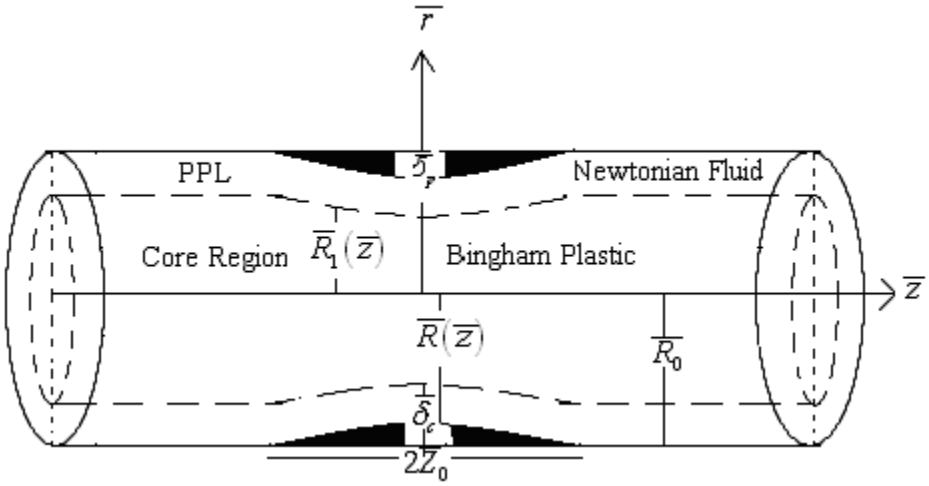

Figure 1. The geometry of an axially symmetric arterial stenosis.

The geometry of the stenosis in the peripheral region is given by

$$\bar{R}(\bar{z}) = \begin{cases} \bar{R}_0 - \dfrac{\bar{\delta}_p}{2}\left(1+\cos\dfrac{\pi\bar{z}}{\bar{z}_0}\right), \text{ for } & |\bar{z}| \le \bar{z}_0, \\ \bar{R}_0, & \text{for } |\bar{z}| > \bar{z}_0. \end{cases} \tag{1}$$

The geometry of the stenosis in the core region is given by

$$\bar{R}_1(\bar{z}) = \begin{cases} \beta\bar{R}_0 - \dfrac{\bar{\delta}_c}{2}\left(1+\cos\dfrac{\pi\bar{z}}{\bar{z}_0}\right), \text{ for } & |\bar{z}| \le \bar{z}_0, \\ \beta\bar{R}_0, & \text{for } |\bar{z}| > \bar{z}_0, \end{cases} \tag{2}$$

where $\bar{R}(\bar{z})$ is the radius of the stenosed artery with peripheral layer; $\bar{R}_1(\bar{z})$ is the radius of the artery in the stenosed core region such that $\bar{R}_1(\bar{z}) = \beta\bar{R}(\bar{z})$; $\bar{R}_0$, $\beta\bar{R}_0$ are the radii the normal artery and core region of the normal artery respectively; $\bar{\delta}_p$ is the maximum height of the stenosis in the peripheral region, β is the ratio of the central core radius to the normal artery radius, $\bar{\delta}_c$ is the maximum height of the stenosis in the core region such that $\bar{\delta}_c = \beta\bar{\delta}_p$ and $\bar{z}_0$ is the half length of the stenosis. It has been reported that the radial velocity is negligibly small for a low Reynolds number flow in a tube with mild stenosis [Nagarani and Sarojamma (2008); Sankar and Lee (2009)]. The equations of motion governing the fluid flow are given by

$$\bar{\rho}_B \frac{\partial \bar{u}_B}{\partial \bar{t}} = -\frac{\partial \bar{p}}{\partial \bar{z}} - \frac{1}{\bar{r}}\frac{\partial}{\partial \bar{r}}\left(\bar{r}\,\bar{\tau}_B\right) + \bar{F}(\bar{t}), \;\; 0 \le \bar{r} \le \bar{R}_1(\bar{z}) \tag{3}$$

$$\bar{\rho}_N \frac{\partial \bar{u}_N}{\partial \bar{t}} = -\frac{\partial \bar{p}}{\partial \bar{z}} - \frac{1}{\bar{r}} \frac{\partial}{\partial \bar{r}} \left(\bar{r} \bar{\tau}_N \right) + \bar{F}\left(\bar{t} \right), \quad \bar{R}_1 \left(\bar{z} \right) \le \bar{r} \le \bar{R}\left(\bar{z} \right) \tag{4}$$

in the core and peripheral regions, respectively, where $\bar{u}_B$, $\bar{u}_N$ are the fluid velocities in the core region and peripheral region respectively; $\bar{\tau}_B$, $\bar{\tau}_N$ are the shear stresses for Bingham plastic fluid and Newtonian fluid respectively; $\bar{\rho}_B$, $\bar{\rho}_N$ are the densities for Bingham plastic fluid and Newtonian fluid respectively; $\bar{p}$ is the pressure and $\bar{F}\left(\bar{t} \right)$ is the body acceleration.

The constitutive equations of Bingham plastic fluid and Newtonian fluid are respectively given by

$$\begin{cases} \bar{\tau}_B = \bar{\tau}_y - \bar{\mu}_B \dfrac{\partial \bar{u}_B}{\partial \bar{r}}, \text{ if } \ \bar{\tau}_B \ge \bar{\tau}_y, \ \bar{R}_p \le \bar{r} \le \bar{R}_1 \left(\bar{z} \right), \\ \dfrac{\partial \bar{u}_B}{\partial \bar{r}} = 0, \qquad \text{if } \bar{\tau}_B \le \bar{\tau}_y, \quad 0 \le \bar{r} \le \bar{R}_p, \end{cases} \tag{5}$$

and

$$\bar{\tau}_N = -\bar{\mu}_N \frac{\partial \bar{u}_N}{\partial \bar{r}} \ \text{ if } \ \bar{R}_1 \left(\bar{z} \right) \le \bar{r} \le \bar{R}\left(\bar{z} \right), \tag{6}$$

where $\bar{R}_p$ is the radius of the plug flow region.

The periodic body acceleration in the axial direction is given by

$$\bar{F}\left(\bar{t} \right) = a_0 \cos\left(\bar{\omega}_b \bar{t} + \phi \right), \tag{7}$$

where a_0 is its amplitude, $\bar{\omega}_b = 2\pi \bar{f}_b$, $\bar{f}_b$ is its frequency in Hz, ϕ is the lead angle of $\bar{F}\left(\bar{t} \right)$ with respect to the heart action. The frequency of body acceleration $\bar{f}_b$ is assumed to be small so that wave effect can be neglected.

The pressure gradient at any $\bar{z}$ and $\bar{t}$ may be represented as follows

$$-\frac{\partial \bar{p}}{\partial \bar{z}} \left(\bar{z}, \bar{t} \right) = A_0 + A_1 \cos\left(\bar{\omega}_p \bar{t} \right), \tag{8}$$

where A_0 is the steady component of the pressure gradient, A_1 is amplitude of the fluctuating component and $\bar{\omega}_p = 2\pi \bar{f}_p$, where $\bar{f}_p$ is the pulse frequency. Both A_0 and A_1 are functions of $\bar{z}$. We introduce the following non-dimensional variables

$$z = \bar{z}/\bar{R}_0,\ R(z) = \bar{R}(\bar{z})/\bar{R}_0, R_1(z) = \bar{R}_1(\bar{z})/\bar{R}_0, r = \bar{r}/\bar{R}_0, t = \bar{t}\,\bar{\omega}_p, \omega = \bar{\omega}_b/\bar{\omega}_p, \delta_p = \bar{\delta}_p/\bar{R}_0,$$

$$\delta_c = \bar{\delta}_c/\bar{R}_0, u_B = \frac{\bar{u}_B}{A_0\bar{R}_0^{\,2}/4\bar{\mu}_B}, u_N = \frac{\bar{u}_N}{A_0\bar{R}_0^{\,2}/4\bar{\mu}_N}, u_s = \frac{\bar{u}_s}{A_0\bar{R}_0^{\,2}/4\bar{\mu}_N}, \tau_B = \frac{\bar{\tau}_B}{A_0\bar{R}_0/2}, \tau_N = \frac{\bar{\tau}_N}{A_0\bar{R}_0/2},$$

$$e = A_1/A_0, B = a_0/A_0, \quad \theta = \frac{\bar{\tau}_y}{A_0\bar{R}_0/2}, \alpha_B^{\,2} = \bar{R}_0^{\,2}\bar{\omega}_p\bar{\rho}_B/\bar{\mu}_B, \alpha_N^{\,2} = \bar{R}_0^{\,2}\bar{\omega}_p\bar{\rho}_N/\bar{\mu}_N, \tag{9}$$

where α_B and α_N are the pulsatile Reynolds numbers for Bingham plastic fluid and Newtonian fluid respectively .

Using non-dimensional variables, equations (1) and (2) become

$$R(z) = \begin{cases} 1 - \dfrac{\delta_p}{2}\left(1 + \cos\dfrac{\pi z}{z_0}\right), & \text{for} \quad |z| \le z_0, \\ 1, & \text{for} \quad |z| > z_0, \end{cases} \tag{10}$$

$$R_1(z) = \begin{cases} \beta - \dfrac{\delta_c}{2}\left(1 + \cos\dfrac{\pi z}{z_0}\right), & \text{for } |z| \le z_0, \\ \beta, & \text{for } |z| > z_0. \end{cases} \tag{11}$$

The governing equations of motion given by equations (3) and (4) are represented in the non-dimensional form as

$$\alpha_B^{\,2}\frac{\partial u_B}{\partial t} = 4f(t) - \frac{2}{r}\frac{\partial}{\partial r}(r\tau_B), \quad 0 \le r \le R_1(z), \tag{12}$$

$$\alpha_N^{\,2}\frac{\partial u_N}{\partial t} = 4f(t) - \frac{2}{r}\frac{\partial}{\partial r}(r\tau_N), \quad R_1(z) \le r \le R(z), \tag{13}$$

where

$$f(t) = (1 + e\cos t) + B\cos(\omega t + \phi), \tag{14}$$

Using non-dimensional variables equations (5) and (6) reduce to

$$\tau_B = \theta - \frac{1}{2}\frac{\partial u_B}{\partial r}, \text{ if } \tau_B \ge \theta, \ R_p \le r \le R_1(z), \tag{15}$$

$$\frac{\partial u_B}{\partial r} = 0, \text{ if } \tau_B \le \theta, \ 0 \le r \le R_p, \tag{16}$$

$$\frac{\partial u_N}{\partial r} = 0, \text{ if } R_1(z) \le r \le R(z). \tag{17}$$

The boundary conditions in the non-dimensional form are given by

$$\text{(i) } \tau_B \text{ is finite at } r = 0, \tag{18}$$

$$\text{(ii) } u_N = u_s \text{ at } r = R(z), \tag{19}$$

$$\text{(iii) } \tau_B = \tau_N, \ u_B = u_N \text{ at } r = R_1(z). \tag{20}$$

The non-dimensional volumetric flow rate is given by

$$Q = 4\int_0^{R(z)} ru(r,z,t)dr, \tag{21}$$

where $Q(t) = \dfrac{\overline{Q}(\overline{t})}{\pi(\overline{R}_0)^4 A_0 / 8\overline{\mu}_B}$; $\overline{Q}(\overline{t})$ is the volumetric flow rate.

The effective viscosity $\overline{\mu}_e$ defined as

$$\overline{\mu}_e = \pi\left(-\frac{\partial \overline{p}}{\partial \overline{z}}\right)\left(\overline{R}(\overline{z})\right)^4 \Big/ \overline{Q}(\overline{t}), \tag{22}$$

can be expressed in dimensionless form as

$$\mu_e = \left(R(z)\right)^4 \left(1 + e\cos t\right) \Big/ Q(t). \tag{23}$$

3. Method of Solution

Since $\alpha_B{}^2, \alpha_N{}^2$ are time dependent, therefore it is necessary to expand equations (12), (13) and (15)-(17) in perturbation series about $\alpha_B{}^2$ and $\alpha_N{}^2$. We expand u_p, R_p and u_N as follows:

$$u_p(z,t) = u_{0p}(z,t) + \alpha_B{}^2 u_{1p}(z,t) + \cdots \tag{24}$$

$$R_p(z,t) = R_{0p}(z,t) + \alpha_B{}^2 R_{1p}(z,t) + \cdots \tag{25}$$

$$u_N(z,r,t) = u_{0N}(z,r,t) + \alpha_N{}^2 u_{1N}(z,r,t) + \cdots \tag{26}$$

Similarly, $u_B, \tau_{B,}\tau_N$ can be expanded in perturbation series in terms of $\alpha_B{}^2$ and $\alpha_N{}^2$. Substituting the perturbation series expansions in equations (12), (15) and (16) and equating powers of $\alpha_B{}^2$, the resulting equations of the core region can be obtained as

$$\frac{\partial}{\partial r}(r\tau_{0B}) = 2f(t)r, \frac{\partial u_{0B}}{\partial t} = -\frac{2}{r}\frac{\partial}{\partial r}(r\tau_{1B}), -\frac{\partial u_{0B}}{\partial r} = 2(\tau_{0B} - \theta), -\frac{\partial u_{1B}}{\partial r} = 2\tau_{1B}. \tag{27}$$

Similarly, using the perturbation series expansions in equations (13) and (17) and equating powers of $\alpha_N{}^2$, the resulting equations of the peripheral region can be obtained as

$$\frac{\partial}{\partial r}(r\tau_{0N}) = 2f(t)r, \frac{\partial u_{0N}}{\partial t} = -\frac{2}{r}\frac{\partial}{\partial r}(r\tau_{1N}), -\frac{\partial u_{0N}}{\partial r} = 2\tau_{0N}, -\frac{\partial u_{1N}}{\partial r} = 2\tau_{1N}. \tag{28}$$

Using perturbation series expansions in equations (18)-(20) and equating constant terms and terms containing $\alpha_B{}^2$ and $\alpha_N{}^2$, we get

τ_{0B} and τ_{1B} are finite at $r = 0$, $\tau_{0B} = \tau_{0N}$, $\tau_{1B} = \tau_{1N}$, $u_{0B} = u_{0N}, u_{1B} = u_{1N}$ at $r = R_1(z)$,

$$u_{0N} = u_s, u_{1N} = 0 \text{ at } r = R(z), \tag{29}$$

On solving equations (27) and (28) for unknowns $u_{0p}, u_{1p}, u_{0B}, u_{1B}, u_{0N}, u_{1N}, \tau_{0B}, \tau_{1B}, \tau_{0N}, \tau_{1N}$ using equation (29), we can obtain,

$$\tau_{0B} = f(t)r, \tau_{0N} = f(t)r, \tag{30}$$

$$u_{0N} = u_s + f(t)\left((R(z))^2 - r^2\right), \tag{31}$$

$$u_{0B} = u_s + f(t)\left((R(z))^2 - r^2\right) - 2kf(t)\left(R_1(z) - r\right), \tag{32}$$

$$u_{0p} = u_s + f(t)\left((R(z))^2 - R_{op}{}^2\right) - 2kf(t)\left(R_1(z) - R_{op}\right), \tag{33}$$

$$\tau_{1B} = -\frac{f'(t)}{24}\left[6(R(z))^2 r - 3r^3 - 4k\left(3R_1(z)r - 2r^2\right)\right], \tag{34}$$

$$\tau_{1N} = -\frac{f'(t)}{24}\left[6\left(R(z)\right)^2 r - 3r^3 - 4k\frac{\left(R_1(z)\right)^3}{r}\right], \tag{35}$$

$$u_{1N} = \frac{f'(t)}{48}\left[12\left(R(z)\right)^2 r^2 - 3r^4 - 9\left(R(z)\right)^4 - 16k\left(R_1(z)\right)^3 \ln\left(\frac{r}{R(z)}\right)\right], \tag{36}$$

$$u_{1B} = \frac{f'(t)}{48}\left[12\left(R(z)\right)^2 r^2 - 3r^4 - 9\left(R(z)\right)^4 - 4k\left\{6R_1(z)r^2 - \frac{8}{3}r^3 - \frac{10}{3}\left(R_1(z)\right)^3 + \left(R_1(z)\right)^3 \ln\left(\frac{R_1(z)}{R(z)}\right)\right\}\right], \tag{37}$$

$$u_{1p} = \frac{f'(t)}{48}\left[12\left(R(z)\right)^2 {R_{0p}}^2 - 3{R_{0p}}^4 - 9\left(R(z)\right)^4 - 4k\left\{6R_1(z){R_{0p}}^2 - \frac{8}{3}{R_{0p}}^3 - \frac{10}{3}\left(R_1(z)\right)^3 + \left(R_1(z)\right)^3 \ln\left(\frac{R_1(z)}{R(z)}\right)\right\}\right], \tag{38}$$

where $k = \theta / f(t)$.

Neglecting the terms of $o\left({\alpha_B}^2\right)$ and higher powers of α_B in equation (25), the first approximation plug-core radius R_{0p} can be obtained as

$$R_{0p} = \theta / f(t) = k\,. \tag{39}$$

Using equations (31), (32), (36) and (37) the expressions for axial velocities in the core and peripheral regions are obtained as

$$u_N = u_s + f(t)\left(\left(R(z)\right)^2 - r^2\right) + \frac{{\alpha_N}^2 f'(t)}{48}\left[12\left(R(z)\right)^2 r^2 - 3r^4 - 9\left(R(z)\right)^4 - 16k\left(R_1(z)\right)^3 \ln\left(\frac{r}{R(z)}\right)\right]. \tag{40}$$

$$u_B = u_s + f(t)\left(\left(R(z)\right)^2 - r^2\right) - 2kf(t)\left(R_1(z) - r\right)$$
$$+\frac{\alpha_B{}^2 f'(t)}{48}\left[12\left(R(z)\right)^2 r^2 - 3r^4 - 9\left(R(z)\right)^4 - 4k\left\{6R_1(z)r^2 - \frac{8}{3}r^3\right.\right.$$
$$\left.\left. - \frac{10}{3}\left(R_1(z)\right)^3 + \left(R_1(z)\right)^3 \ln\left(\frac{R_1(z)}{R(z)}\right)\right\}\right]. \tag{41}$$

Similarly, using equations (24), (33) and (38), the expression for plug-core velocity can easily be obtained.

The expression for wall shear stress τ_w can be obtained by

$$\tau_w = \left(\tau_{0N} + \alpha_N{}^2 \tau_{1N}\right)_{r=R(z)}, \tag{42}$$
$$= f(t)R(z) - \frac{\alpha_N{}^2 f'(t)}{24}\left[3\left(R(z)\right)^3 - 4k\frac{\left(R_1(z)\right)^3}{R(z)}\right]. \tag{43}$$

From equations (21), (40) and (41) the volumetric flow rate is given by

$$Q = 4\int_0^{R_{0p}} r\left(u_{0p} + \alpha_B{}^2 u_{1p}\right)dr + 4\int_{R_{0p}}^{R_1(z)} r\left(u_{0B} + \alpha_B{}^2 u_{1B}\right)dr + 4\int_{R_1(z)}^{R(z)} r\left(u_{0N} + \alpha_N{}^2 u_{1N}\right)dr$$

$$= 2u_s R^2 + f(t)\left[R^4 - R_{0p}{}^4 - \frac{4k^2}{3}\left(R_1{}^3 - R_{0p}{}^3\right)\right]$$

$$+\frac{f'(t)\alpha_B{}^2}{24}\left[6R^2 R_{0p}{}^4 - 2R_{0p}{}^6 - R_1{}^6 + 6R^2 R_1{}^4 - 9R^4 R_1{}^2 - 4k\left\{3R_1 R_{0p}{}^4 - \frac{8}{5}R_{0p}{}^5 - \frac{7}{5}R_1{}^5 + R_1{}^5 \ln\left(\frac{R_1}{R}\right)\right\}\right]$$

$$+\frac{f'(t)\alpha_N{}^2}{24}\left[9R^4 R_1{}^2 - 6R^2 R_1{}^4 - 4R^6 + R_1{}^6 + 8k\left\{2R_1{}^5 \ln\left(\frac{R_1}{R}\right) + R^2 R_1{}^3 - R_1{}^5\right\}\right], \tag{44}$$

where $R = R(z)$, $R_1 = R_1(z)$. The expression for effective viscosity μ_e can be obtained from equations (23) and (44).

The second approximation plug core radius R_{1p} can be obtained by neglecting terms of $o\left(\alpha_B{}^4\right)$ and higher powers of α_B in equation (28) as

$$R_{1p} = \frac{-\tau_{1B}\left(R_{0p}\right)}{f\left(t\right)}$$

$$= -\frac{f'\left(t\right)k^2}{24}\left(6R^2 - 5k - 12R_1\right). \tag{45}$$

From equations (25), (39) and (45), the expression for plug-core radius can be obtained as

$$R_p = k - \frac{\alpha_B{}^2 f'\left(t\right)k^4}{24}\left(6R^2 - 5k^2 - 12R_1\right). \tag{46}$$

In absence of yield stress $\left(\text{i.e.,}\theta = 0\right)$ and peripheral plasma layer $\left(\text{i.e.,}\ \beta = 1, R\left(z\right) = R_1\left(z\right)\right)$ the flow system represented by the equations (40)-(44) reduce to one-layered Newtonian flow system with body acceleration as

$$u = u_s + f\left(t\right)\left(\left(R\left(z\right)\right)^2 - r^2\right) + \frac{\alpha^2}{16} f'\left(t\right)\left(4\left(R\left(z\right)\right)^2 r^2 - 3\left(R\left(z\right)\right)^4 - r^4\right), \tag{47}$$

$$Q = \left(R\left(z\right)\right)^2\left\{2u_s + f\left(t\right)\left(R\left(z\right)\right)^2 - \frac{\alpha^2}{6} f'\left(t\right)\left(R\left(z\right)\right)^4\right\}, \tag{48}$$

$$\tau_w = f\left(t\right)R\left(z\right) - \frac{\alpha^2}{8} f'\left(t\right)\left(R\left(z\right)\right)^3, \tag{49}$$

$$\mu_e = \left(R\left(z\right)\right)^2\left(1 + e\cos t\right)\left\{2u_s + f\left(t\right)\left(R\left(z\right)\right)^2 - \frac{\alpha^2}{6} f'\left(t\right)\left(R\left(z\right)\right)^4\right\}^{-1}. \tag{50}$$

The results given by equations (47)-(50) are the results obtained in Biswas and Chakraborty (2009a).

4. Results and Discussions

The present model has been developed to analyze the combined effects of body acceleration; stenosis and velocity slip on the flow variables viz., axial velocity, flow rate, shear stress and effective viscosity of blood, flowing in an artery with a mild constriction. The equations governing the abovementioned flow are integrated by using a perturbation analysis with very small Womersley frequency parameters ($\alpha_B = \alpha_N = 0.5 < 1$). The pressure gradient parameter e is taken in the range 0-5, the body acceleration parameter B is taken in the range 0-2, magnitude of the lead angle ϕ is taken as 0.2 and the range 0-0.5 is taken for the height of the stenosis δ_p in the

peripheral region. The axial velocity slip u_s is considered from 0 to 0.1, the ratio β of the central core radius to the normal radius of the artery is taken as 0.8, yield stress is taken as 0, 0.1 and the magnitude of z is taken from -4 to 4.

The variation of axial velocity, using equations (40) and (41) at the throat of the stenosis (i.e. at z =0) with radial distance, for fixed values of peripheral stenosis height δ_p, pressure gradient e, time t and for different values of slip velocity u_s and body acceleration parameter B, are presented in Figure 2.

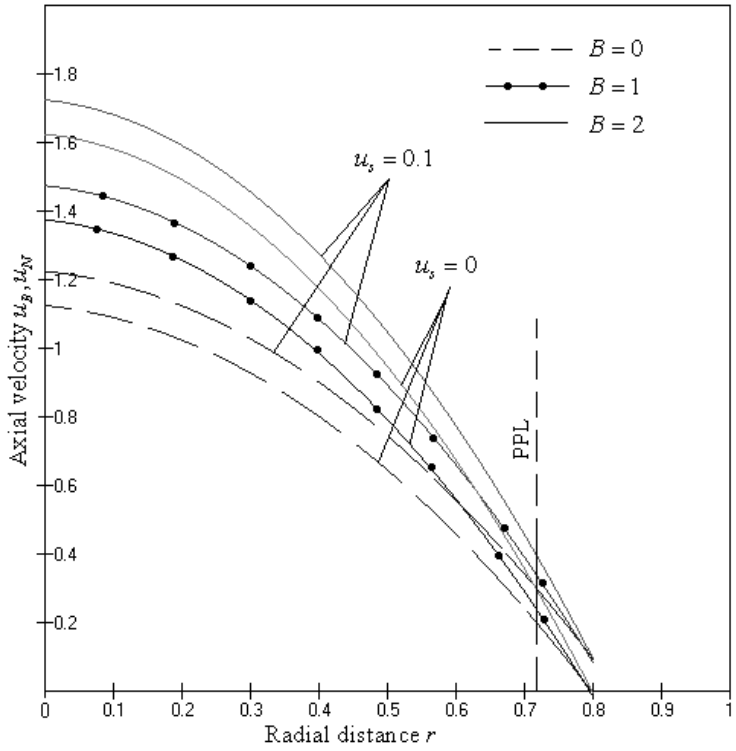

Figure 2: Variation of axial velocity with radial distance r for $t = 45^0$, $e = 1$, $\delta_p = 0.2$, $B = 1, z = 0, \beta = 0.8$ and for different values of z and u_s

It is observed from the figure that axial velocity is maximum at $r = 0$, wherefrom it gradually decreases with the increase in radius of the artery r and attains a minimum value at the stenotic wall ($r = R(z)$) for any value of body acceleration parameter B. However, an employment of slip at the wall increases the axial velocity. Increase in body acceleration further enhances the axial velocity.

Variation of volumetric flow rate with the pressure gradient parameter e for fixed values of peripheral stenosis height δ_p, time t and for different values of slip velocity u_s, yield stress θ and

body acceleration parameter B, are depicted in Fig. 3. It is observed that flow rate gradually increases with the increase in pressure gradient parameter e for any value of B and θ. However, the magnitude of flow rate in the absence of yield stress ($\theta = 0$) is more than its magnitude in presence of yield stress. It is further noticed that employment of body acceleration enhances the flow rate.

Variation of Wall shear stress with axial distance z and time t are presented in Fig. 4 and Fig. 5 respectively. Form the figures, it can be clearly observed that wall shear stress τ_w increases from its approached magnitude (i.e. at $z = -4$)in the upstream of the throat with the axial distance and achieves its maximal at the throat of the stenosis and then decreases in the downstream and attains a lower magnitude at the end of the constriction profile (i.e. at $z = 4$). Magnitude of wall shear stress τ_w in uniform tube ($\delta_p = 0$) is lower than its magnitude in stenosed artery ($\delta_p > 0$). It increases significantly with the height of the peripheral stenosis δ_p for any value of body acceleration parameter B. However, body acceleration decreases wall shear stress in both uniform ($\delta_p = 0$) and stenosed ($\delta_p > 0$) arteries.

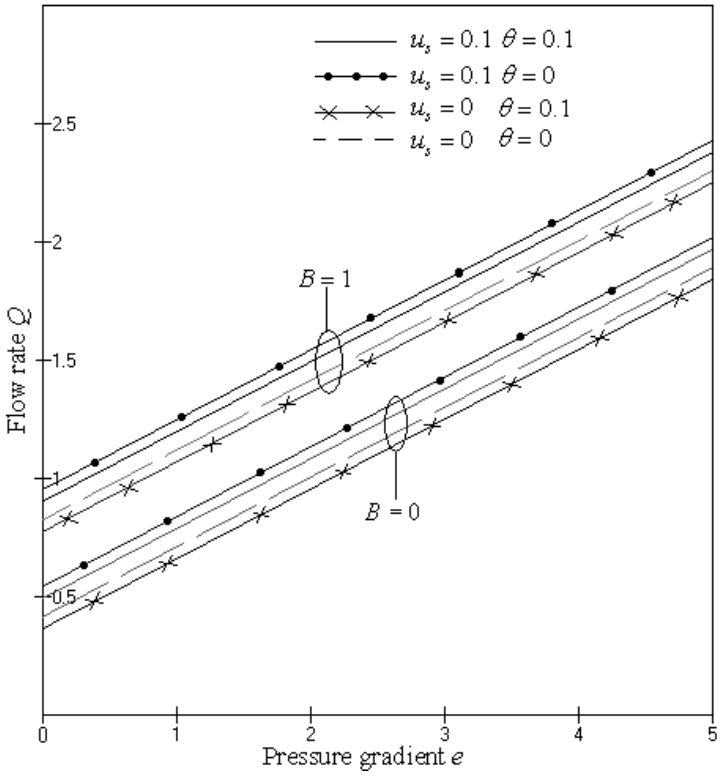

Figure 3. Variation of flow rate with pressure gradient for $B = 1, \delta_p = 0.2, t = 45^0, z = 0, \beta = 0.8$

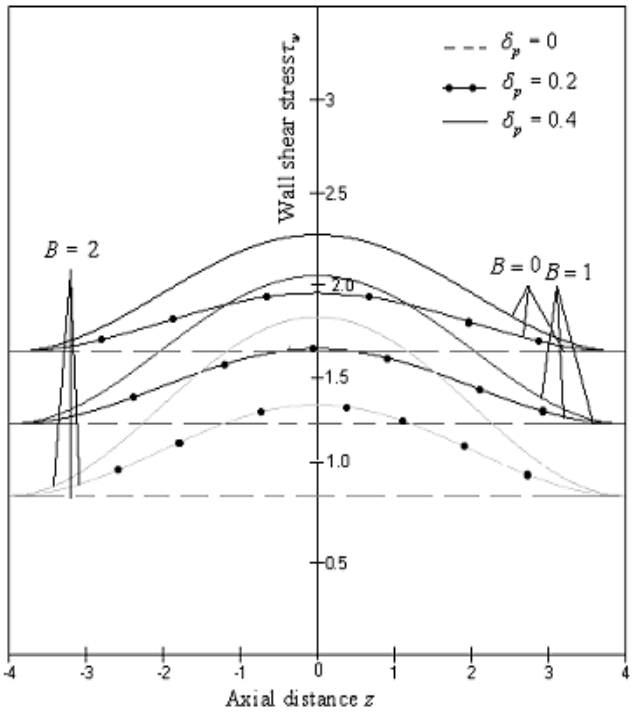

Figure 4. Variation of wall shear stress with axial distance for $\theta = 0.1, t = 180^0, z = 0, \beta = 0.8$

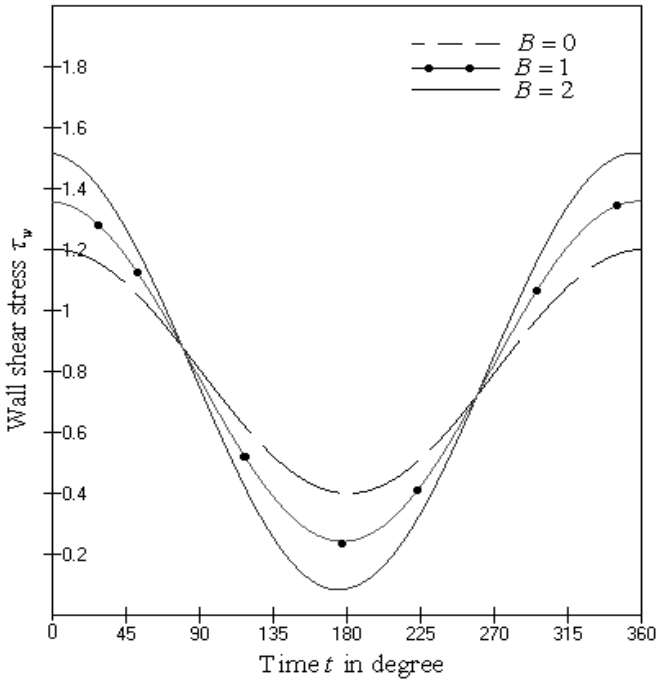

Figure 5. Variation of wall shear stress with axial distance for $\theta = 0.1, \beta = 0.8, z = 0$

It is also noticed that for any value of body acceleration parameter B, wall shear stress τ_w gradually decreases as time t increases until it attains its minimum at $t = 180^0$, wherefrom it gradually increases with time and reaches its approached magnitude at $t = 360^0$.

Variation of effective viscosity μ_e with axial distance z and peripheral stenosis height δ_p are presented graphically in Figure 6 and Figure 7, respectively.

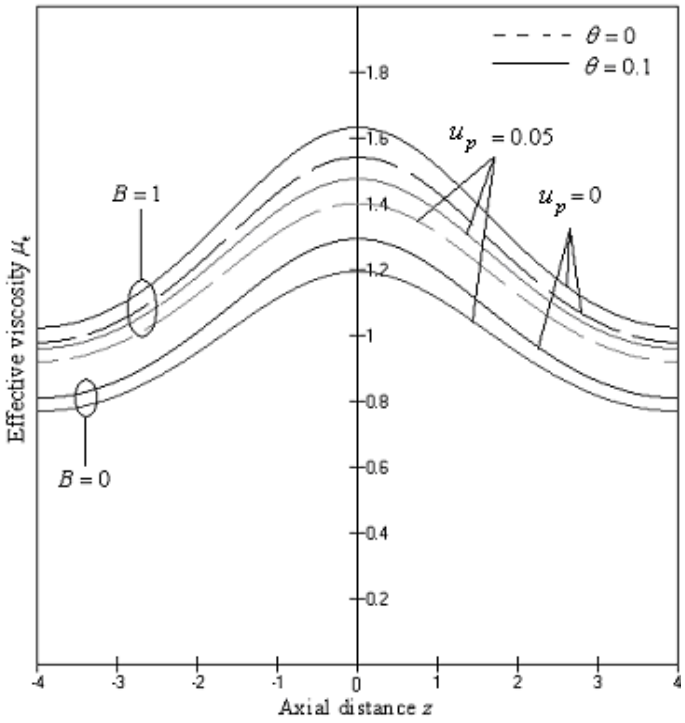

Figure 6. Variation of effective viscosity with axial distance for $t = 45^0, \beta = 0.8, z = 0$

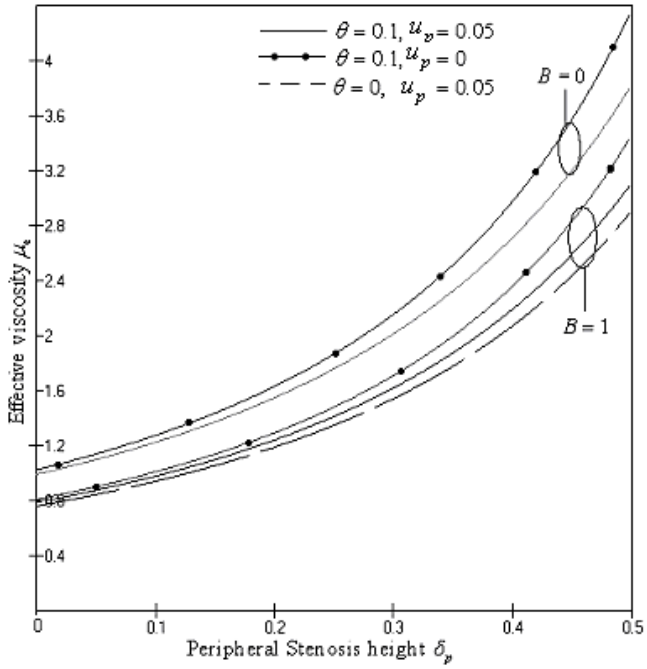

Figure 7. Variation of effective viscosity with peripheral stenosis height for $t = 45^0, \beta = 0.8, z = 0$

Effective viscosity increases with the axial distance z from the initiation of a stenosis (i.e. at $z = -4$) till it reaches to its maximum value at the throat (i.e. at $z = 0$), wherefrom it gradually decreases to its initial value at the termination of the stenosis (i.e., at $z = 4$). It is also observed from the figures that effective viscosity μ_e increases with peripheral stenosis height for both the cases of no-slip and slip at wall. However, for any value of body acceleration parameter B, employment of an axial slip velocity at wall reduces the effective viscosity both in presence and absence of yield stress. For fixed values of B and u_s, effective viscosity increases with yield stress.

5. Conclusion

The present analysis deals with the two-layered pulsatile blood flow through an artery (Fig.1) embedded with an axi-symmetric mild stenosis and an axial velocity slip is employed at the constricted wall. The body fluid blood is assumed to behave like a Newtonian fluid in the peripheral plasma layer and it is represented as Bingham Plastic in the core region. The equations of motion, governing the flow are integrated by using a perturbation method. Analytic expressions for flow variables are obtained and their variations with different flow parameters are presented graphically. It is observed that as expected, axial velocity and flow rate increase with the wall slip whereas effective viscosity decreases due to a slip. Also wall shear stress and effective viscosity decrease but velocity and flow rate increase with the body acceleration parameter B .Effective viscosity μ_e increases as δ_p increases.

However, μ_e is lowered for both the uniform tube $\left(\delta_p = 0\right)$ and stenosed artery $\left(\delta_p > 0\right)$, as a result of wall slip. Since this study, takes care of pulsatility of the flow and also it incorporates the characteristics of non-Newtonian nature of blood (which is prominent in case of flow through arteries with smaller diameter), it is strongly felt that the present model may provide a better insight to the study of blood flow. This model indicates that slip at a diseased artery could play a prominent role in blood flow modeling. From the analysis, it may also be concluded that with slip, the damages to the vessel wall could be reduced. This kind of reduction in wall shear stress and effective viscosity could be exploited for better functioning of the diseased arterial systems. Hence one may look forward for drugs or devices which would produce slip and use them for treatment of peripheral arterial diseases. Further improvement in the model could be done by considering permeability of the blood vessels.

Acknowledgements

Authors express sincere thanks to Prof. A. M. Haghighi, the Editor-in-Chief and the reviewers of the journal for their valuable comments. They are also grateful to Dr. Sudip Choudhury, Assam University, Silchar, India for valuable discussions.

REFERENCES

Bali, R. and Awasthi, U. (2007). Effect of a Magnetic Field on the Resistance to Blood Flow through Stenosed Artery, Appl. Math. Comput., Vol. 188, pp.1635-1641.

Bennet, L. (1967). Red Cell Slip at a Wall *in vitro*, Science, Vol. 155, pp.1554-1556.

Biswas, D. (2000). Blood Flow Models: A Comparative Study, Mittal Publications, New Delhi.

Biswas, D. and Chakraborty, U.S. (2009a). Pulsatile Flow of Blood in a Constricted Artery with Body Acceleration, Appl. Appl. Math., Vol. 4(2), pp. 329-342.

Biswas, D. and Chakraborty, U.S. (2009b). Pulsatile Flow of Blood in a Constricted Artery with a Velocity Slip, Far East Journal of Applied Mathematics, Vol. 36(3), pp. 331-342.

Biswas, D. and Chakraborty, U.S. (2010). Pulsatile Blood Flow through a Catheterized Artery with an Axially Nonsymmetrical Stenosis, Applied Mathematical Sciences, Vol. 4(58), pp. 2865-2880.

Brunn, P. (1975). The Velocity Slip of Polar Fluids, Rheol. Acta., Vol. 14, pp.1039-1054.

Bugliarello, G. and Sevilla, J. (1970).Velocity Distribution and Other Characteristics of Steady and Pulsatile Blood Flow in Fine Glass Tubes, Biorheology, Vol.7, pp. 85-107.

Chaturani, P. and Upadhya, V. S. (1979).On Micropolar Fluid Model for Blood Flow through Narrow Tubes, Biorheology, Vol. 16, pp. 419-428.

Chaturani, P. and Upadhya, V. S. (1981). A Two-Fluid Model for Blood Flow through Small Diameter Tubes with Non-Zero Couple Stress Boundary Condition at the Interface, Biorheology, Vol.18, pp. 245-253.

Chaturani, P. and Biswas, D. (1984**).** A Comparative Study of Poiseuille Flow of a Polar Fluid Under Various Boundary Conditions with Applications to Blood Flow, Rheol. Acta., Vol. 23, pp. 435-445.

Chaturani, P. and Samy, R.P. (1985). A Study of Non-Newtonian Aspects of Blood Flow through Stenosed Arteries and its Applications in Arterial Diseases, Biorheology, Vol. 22, pp. 521-531.

Charm, S.E. and Kurland, G.S. (1974). Blood Flow and Micro Circulation, John Wiley, New York.

Cokelet, G. R. (1972). The Rheology of Human Blood: In Biomechanics (Ed. Y.C. Fung et al.), Prentice Hall, Englewood Cliffs, New Jersey.

Day, M.A. (1990). The No-Slip Condition of Fluid Dynamics. Erkenntnis, Vol. 33, 285-296.

Fung, Y.C. (1981). Biomechanics: Mechanical Properties of Living Tissues, Springer-Verlag, New York.

Guyton, A.C. and Hall, J.E. (2006). Textbook of Medical Physiology, Elsevier.

Jones, A.L. (1966). On the Flow of Blood in a Tube. Biorheology, Vol. 3, pp. 183-188.

Kapur, J.N., Bhat, B.S. and Sacheti, N.C. (1982). Non-Newtonian Fluid Flows (A Survey Monograph), Pragati Prakashan, Meerut.

McDonald, D.A. (1979). On Steady Flow through Modeled Vascular Stenosis, J. Biomech., Vol. 12, pp.13–20.

Mandal, P.K. (2005). An Unsteady Analysis of Non-Newtonian Blood Flow through Tapered Arteries with a Stenosis, Int. J. Nonlinear Mech., Vol. 40, pp.151-164.

Merrill, E.W. (1965). Rheology of Human Blood and Some Speculations on its Role in Vascular Homeostasis Biomechanical Mechanisms in Vascular Homeostasis and Intravascular Thrombosis, P.N. Sawyer (ed.), Appleton Century Crofts, New York, pp.127-137.

Misra, J.C. and Shit, G.C. (2007). Role of Slip Velocity in Blood Flow through Stenosed Arteries: A Non-Newtonian Model, Journal of Mechanics in Medicine and Biology, Vol. 7, pp. 337-353.

Misra, J.C., Adhikary, S.D. and Shit, G.C. (2008). Mathematical Analysis of Blood Flow through an Arterial Segment with Time-dependent Stenosis, Mathematical Modeling and Analysis. Vol. 13, pp. 401-412.

Nagarani, P. and Sarojamma, G. (2008). Effect of Body Acceleration on Pulsatile Flow of Casson Fluid through a Mild Stenosed Artery, Korea-Australia Rheology Journal, Vol. 20, pp.189-196.

Nubar, Y. (1967). Effects of Slip on the Rheology of a Composite Fluid: Application to Blood Flow, Rheology, Vol. 4, pp.133-150.

Ponalgusamy, R. (2007). Blood flow through an artery with mild stenosis: A Two-Layered Model, Different Shapes of Stenoses and Slip Velocity at the Wall. Journal of Applied Sciences, Vol. 7, pp. 1071-1077.

Sankar, D.S. and Ismail, A.I.M. (2009). Two-Fluid Mathematical Models for Blood Flow in Stenosed Arteries: A Comparative Study, Boundary Value Problems, Vol. 2009, 568657.

Sankar, D.S. and Lee, U. (2009). Mathematical Modeling of Pulsatile Flow of Non-Newtonian Fluid in Stenosed Arteries. Commun. Nonlinear. Sci. Numer. Simulat., Vol. 14, pp. 2971-2981.

Schlicting, H. (1968). Boundary Layer Theory, McGraw- Hill Book Company, New York.

Shukla, J. B., Parihar, R. S. and Gupta, S. P. (1980). Effects of Peripheral Layer Viscosity on Blood Flow through an Artery with Mild Stenosis. Bulletin of Mathematical Biology, Vol. 42, pp. 797-805.

Sinha, P. and Singh, C. (1984). Effects of Couple Stresses on the Blood Flow through an Artery with Mild Stenosis, Biorheology, 21, pp. 303-315.

Srivastava, V. P. (2000). Blood Flow through Stenosed Vessels with a Peripheral Plasma Layer and Applications. Automedica, Vol. 18, pp. 271-300.

Sud, V.K. and Sekhon, G. S. (1985). Arterial Flow Under Periodic Body Acceleration, Bulletin of Mathematical Biology, Vol. 47, pp. 35-52.

Sud, V.K. and Sekhon, G. S. (1987). Flow through a Stenosed Artery Subject to Periodic Body Acceleration, Med. Biol. Eng. & Comput., Vol. 25**,** pp. 638- 644.

Taylor, M.G. (1959). The Influence of Anomalous Viscosity of Blood upon its Oscillatory Flow. Physics in Medicine and Biology, Vol. 3, pp. 273-290.

Vand, V. (1948). Viscosity of Solutions and Suspensions, J. Phys. Colloid. Chem. Vol. 52, pp. 277-321.

Young, D. F. (1968). Effects of a Time-Dependent Stenosis of Flow through a Tube, Journal of Eng. Ind., Vol. 90, pp. 248-254.